Title

Evidence of mixing between polluted convective outflow and stratospheric air in the upper troposphere during DC3

Journal

Journal of Geophysical Research, 119(19)

ISSN

0148-0227

Authors

Schroeder, JR
Pan, LL
Ryerson, T
et al.

Publication Date

2014-10-16

DOI

10.1002/2014JD022109

AGU PUBLICATIONS

JGR

Journal of Geophysical Research: Atmospheres

RESEARCH ARTICLE
10.1002/2014JD022109

Special Section:
Deep Convective Clouds and Chemistry 2012 Studies (DC3)

Evidence of mixing between polluted convective outflow and stratospheric air in the upper troposphere during DC3

Jason R. Schroeder[1], Laura L. Pan[2], Tom Ryerson[3], Glenn Diskin[4], Johnathan Hair[4], Simone Meinardi[1], Isobel Simpson[1], Barbara Barletta[1], Nicola Blake[1], and Donald R. Blake[1]

[1]Department of Chemistry, University of California-Irvine, Irvine, California, USA, [2]National Center for Atmospheric Research, Boulder, Colorado, USA, [3]Earth System Research Laboratory, National Oceanic and Atmospheric Administration, Boulder, Colorado, USA, [4]NASA Langley Research Center, Hampton, Virginia, USA

Key Points:
- VOCs used to tag stratospheric air masses
- Evidence suggests that stratospheric air can mix with convective outflow

Correspondence to:
J. R. Schroeder,
schroedj@uci.edu

Citation:
Schroeder, J. R., L. L. Pan, T. Ryerson, G. Diskin, J. Hair, S. Meinardi, I. Simpson, B. Barletta, N. Blake, and D. R. Blake (2014), Evidence of mixing between polluted convective outflow and stratospheric air in the upper troposphere during DC3, *J. Geophys. Res. Atmos.*, *119*, 11,477–11,491, doi:10.1002/2014JD022109.

Received 30 MAY 2014
Accepted 2 SEP 2014
Accepted article online 4 SEP 2014
Published online 7 OCT 2014

Abstract Aircraft measurements, including non-methane hydrocarbons (NMHCs), long-lived halocarbons, carbon monoxide (CO), and ozone (O_3) collected on board the NASA DC-8 during the Deep Convection, Clouds, and Chemistry (DC3) field campaign (May – June 2012), were used to investigate interactions and mixing between stratospheric intrusions and polluted air masses. Stratospherically influenced air masses were detected using a suite of long-lived halocarbons, including chlorofluorocarbons (CFCs) and HCFCs, as a tracer for stratospheric air. A large number of stratospherically influenced samples were found to have reduced levels of O_3 and elevated levels of CO (both relative to background stratospheric air), indicative of mixing with anthropogenically influenced air. Using *n*-butane and propane as further tracers of anthropogenically influenced air, we show that this type of mixing was present both at low altitudes and in the upper troposphere (UT). At low altitudes, this mixing resulted in O_3 enhancements consistent with those reported at surface sites during deep stratospheric intrusions, while in the UT, two case studies were performed to identify the process by which this mixing occurs. In the first case study, stratospheric air was found to be mixed with aged outflow from a convective storm, while in the second case study, stratospheric air was found to have mixed with outflow from an active storm occurring in the vicinity of a stratospheric intrusion. From these analyses, we conclude that deep convective events may facilitate the mixing between stratospheric air and polluted boundary layer air in the UT. Throughout the entire DC3 study region, this mixing was found to be prevalent: 72% of all samples that involve stratosphere-troposphere mixing show influence of polluted air. Applying a simple chemical kinetics analysis to these data, we show that during DC3, the instantaneous production of hydroxyl radical (OH) in these mixed stratospheric-polluted air masses was 11 ± 8 times higher than that of stratospheric air, and 4.2 ± 1.8 times higher than that of background upper tropospheric air.

1. Introduction

The Earth's stratosphere is a large reservoir of ozone (O_3), which shields life from the Sun's harmful ultraviolet radiation. In contrast, tropospheric O_3 is a key component of photochemical smog and can cause respiratory problems in humans and harm to vegetation, and can alter the oxidizing capacity of an air mass via photochemical production of the hydroxyl radical (OH) [*Crutzen and Zimmerman*, 1991; *Michelsen et al.*, 1994; *WHO*, 2005]. Stratosphere-to-troposphere transport (STT) commonly occurs at middle latitudes to high latitudes during late winter and spring, and can transport large amounts of O_3 to both the upper and lower troposphere [*Büker et al.*, 2008; *Avery et al.*, 2010; *Langford et al.*, 2012; *Lin et al.*, 2012]. Although not well characterized, STT events are known to often occur in the vicinity of convective events, which can result in mixing of stratospheric air with convectively lofted air from the lower troposphere, including polluted air from the planetary boundary layer (PBL) [*Cho et al.*, 2001; *Stohl*, 2003; *Colette and Ancellet*, 2006; *Homeyer et al.*, 2011]. This mixing may in turn affect the oxidizing capacity of the upper troposphere (UT), and the lifetime of trace gases in convective outflow. Local-scale measurements of the transportation and mixing of stratospheric air with air from the PBL prove difficult to obtain —some of the key characteristics of stratospheric air can become masked by polluted air, making detection and characterization difficult [*Stohl et al.*, 2003]. In this paper, we investigate STT in the vicinity of convective storms and the time scale and extent to which mixing between stratospheric air and convective outflow occurs. To do this, a tracer for stratospheric air is developed from in situ measurement of long-lived halocarbons during the Deep Convection, Clouds, and Chemistry (DC3) field campaign, which took place over the central US in spring 2012.

Stratosphere-to-troposphere transport (STT) commonly occurs at middle latitudes to high latitudes as part of a general large-scale downward mass flux, and its impact on regional and global tropospheric O_3 has been studied [*Büker et al*., 2008; *Avery et al*., 2010; *Langford et al*., 2012; *Lin et al*., 2012]. The average depth to which stratospheric air masses penetrate into the extratropical troposphere has a seasonal variation, with the deepest STT events occurring in winter and spring [*Stohl*, 2003]. Extratropical STT events are associated with synoptic-scale and mesoscale processes, including the formation of tropopause folds in the vicinity of polar and subtropical jet streams [*Vaughan et al*., 1994; *Langford et al*., 1996], erosion and folding of the tropopause by convective activity near cut-off-lows [*Price and Vaughan*, 1993; *Ancellet and Beekmann*, 1994; *Sprenger et al*., 2007], mesoscale convective systems [*Poulida et al*., 1996], and isolated convective storms [*Cho et al*., 2001; *Stohl*, 2003; *Colette and Ancellet*, 2006; *Pan et al*., 2014]. From this, it can be inferred that STT in the extratropics is sporadic in nature and generally associated with unstable meteorological conditions, often in the immediate vicinity of convection. Convective storms are also sporadic in nature but have peak activity over the continental United States during spring and summer [*Carbone et al*., 2002]. Deep convective storms can rapidly transport air from the PBL to the upper troposphere/lower stratosphere (UT/LS) region, with observed transport times ranging from 15 to 120 min [*Aschmann et al*., 2009; *Apel et al*., 2012]. This rapid transport affects the composition of the UT by injecting short-lived trace gases, aerosols, and water vapor, which in turn affects the chemistry of the UT.

On a global scale, 30–50% of O_3 in the UT is believed to have originated from the stratosphere and, through photochemical reactions in the presence of water vapor, is the dominant natural source of OH in the troposphere [*Crutzen et al*., 1999; *Fusco*, 2003]. The photochemical reactions that produce OH from O_3 are shown below:

$$\mathbf{O_3 + h\nu \xrightarrow{k_1} O_2 + O(^1D)} \quad \boldsymbol{h\nu < 320\ nm} \tag{1}$$

Upon absorption of ultraviolet light, O_3 molecules dissociate (with photolysis rate constant k_1) into molecular oxygen and electronically excited atomic oxygen (reaction (1)). Electronically excited oxygen atoms can then relax to their ground state upon collision with spectator molecules (M), with rate constant k_2 (reaction (2)).

$$\mathbf{O(^1D) + M \xrightarrow{k_2} O(^3P) + M} \tag{2}$$

Ground state oxygen atoms may react with molecular oxygen in the presence of spectator molecules to re-form O_3, with rate constant k_3 (reaction (3)),

$$\mathbf{O(^3P) + O_2 + M \xrightarrow{k_3} O_3} \tag{3}$$

However, electronically excited oxygen atoms can also react with molecules of water vapor, producing two OH radicals with rate constant k_4 (reaction (4)).

$$\mathbf{O(^1D) + H_2O \xrightarrow{k_4} 2OH} \tag{4}$$

Assuming steady state condition for $O(^1D)$ and $k_2 >> k_4$, the instantaneous production of OH (P_{OH}) can be simplified to:

$$\mathbf{P_{OH}} = \frac{\mathbf{2k_1k_4}}{\mathbf{k_2[M]}}\mathbf{[O_3][H_2O]} \tag{5}$$

Stratospheric intrusions that have recently entered the UT have high levels of O_3 and low levels of water vapor, while convectively lofted lower-tropospheric air will have relatively low levels of O_3 and high levels of water vapor [*Bithell et al*., 2000]. As predicted by equation (5), mixing between high-O_3 stratospheric air and moist tropospheric air will result in an increased production of OH and therefore a reduction in the lifetimes of volatile organic compounds (VOCs) that are co-lofted into the UT with the water vapor, since the lifetimes of many VOCs are directly proportional to OH mixing ratios [*Poisson et al*., 2000; *Aschmann et al*., 2009; *Apel et al*., 2012]. As stratospheric O_3 levels continue to recover due to regulation of chlorofluorocarbons (CFCs) and other O_3-depleting substances, the impact of STT may become even larger in the coming decades [*Zeng et al*., 2010].

Due to their high levels of O_3 and low levels of water vapor and CO, pristine stratospheric intrusions are relatively easy to detect by ground-based lidar and simple in situ surface and airborne-based measurements [*Fenn et al*., 1999; *Bithell et al*., 2000; *Vaughan et al*., 2001; *Browell*, 2003; *Langford et al*., 2012; *Lin et al*., 2012]. After mixing with relatively polluted air, detection of stratospheric influence becomes more difficult, since O_3

will be diluted and the introduction of water vapor, CO, and VOCs effectively acts to mask the stratospheric character [*Stohl et al.*, 2003]. The cosmogenic nuclide ^{7}Be has often been used as a tracer for stratospheric air, but its usefulness is questionable as it is estimated that a third of all ^{7}Be originates in the UT and is removed by deposition onto aerosols and wet scavenging [*Dibb et al.*, 1994; *Koch and Mann*, 1996; *Gerasopoulos et al.*, 2001; *Doering and Akber*, 2008]. Furthermore, ^{7}Be was not measured during DC3. However, certain anthropogenic halocarbons, including long-lived species like CFCs and their replacement HCFCs, are only photochemically destroyed in the stratosphere and (as a result of the Montreal Protocol) currently have minimal surface sources, even on a global scale [*World Meteorological Organization*, *WMO/United Nations Environment Programme*, *UNEP*, 2007]. As a result, these halocarbons are evenly distributed throughout the troposphere, but relatively depleted in the stratosphere—making them ideal tracers for stratospheric air. Nitrous oxide (N_2O) is also solely destroyed in the stratosphere and has been used as a tracer for stratospheric air but has some properties that make it non-ideal for this particular application [*Ishijima et al.*, 2010; *Assonov et al.*, 2013]. Tropospheric N_2O mixing ratios continue to increase at a rate of ~ 1 ppbv per year due to surface sources including agricultural and industrial sources [*Hartmann et al.*, 2013]. This means that, upon mixing, the N_2O-depleted character of stratospheric air may be masked by the N_2O-enhanced character of PBL air. This would be especially problematic if the boundary layer air from a region with strong N_2O sources was to be convectively lofted and mixed. Thus, while N_2O is an effective tracer for stratospheric intrusions, the use of long-lived halocarbons with minimal surface sources as tracers for stratospheric air is better suited for this work. By contrast, relatively short-lived gases such as biogenic VOCs and long-chained hydrocarbons have significant surface sources and very strong tropospheric gradients, making them useful tracers for fresh vertical convection.

Based in Salina, Kansas (GPS coordinates: 38.8403, −97.6114) from May to June 2012 (local time = UTC − 05:00), the Deep Convective Clouds and Chemistry (DC3) project was a collaborative, multi-agency, multi-platform campaign whose primary objective was to study the chemical and transport processes associated with deep convection. Of particular interest was the transport and chemical transformation of air from the PBL to the free troposphere (FT) and UT via deep convection. In the work presented below, the spatial and temporal trends of stratospheric intrusions during DC3 are investigated, with a particular emphasis on events where stratospheric air mixed with the high-altitude outflow from convective storms. Potential impacts on convective outflow and upper tropospheric chemistry are also investigated.

2. Experimental

During the DC3 field campaign, UC Irvine's whole air sampler (WAS) was stationed aboard the NASA DC-8 research aircraft and used to collect 1795 samples during 18 research flights. Active convective storms were sampled in the three regions where ground-based radar support was available—Northern Alabama; near the Texas/Oklahoma border; and above the high plains near the Colorado/Wyoming/Nebraska border. Of the 18 research flights flown during DC3, 14 had a primary objective of analyzing active convective storms in one of these three regions. The four remaining flights focused on tracking aged outflow from storms that had occurred the previous day. WAS sample collection on the NASA DC-8 aircraft was controlled using a dual head metal bellows pump connected to a 0.25″ forward-facing inlet on the outside of the aircraft. Air was collected into evacuated, pre-conditioned 2 L stainless steel canisters that were manually opened and closed using a metal bellows valve.

Prior to use, all canisters were pre-conditioned by the following process to ensure measurement reproducibility: First, all canisters underwent a pump-and-flush procedure ten times with air collected at White Mountain (altitude 10,200 feet) in the Sierra Nevada mountains. Next, all canisters were evacuated to 10^{-2} Torr then flushed with ultra-high-purity helium. After venting the helium, all canisters were again evacuated to 10^{-2} Torr. All canisters were then sealed for 2 weeks, after which they were checked for leaks. Finally, 17 Torr of purified water vapor was added to each canister to minimize gas adsorption onto the interior surface of our canisters. Sensitivity tests have shown that, following this procedure, VOC mixing ratios remain stable in our canisters for 1–2 weeks, and the only compounds that are lost in any appreciable amount are the heavier hydrocarbons (i.e., C_8 and higher alkanes, terpenes, etc.) [*Sive*, 1998].

Table 1. Gases Used as Tracers of Stratospheric Air

Gas	Formula	Lifetime[a]	Measurement Precision (%)	Min (pptv)	Max (pptv)	Avg (pptv)	25th percentile value (pptv)
CFC-11	CCl_3F	45 years	1	209	250	240.8	237
CFC-12	CCl_2F_2	100 years	1	238	557	541.3	536
HCFC-22	CHF_2Cl	11.9 years	1	216.4	278.9	247.7	241.2
HCFC-141b	CH_3CCl_2F	9.2 years	5	17.3	31.1	23.6	21.4
HCFC-142b	CH_2ClCF_2	17.2 years	3	19.7	26.5	22.6	21.1
Carbon Tetrachloride	CCl_4	26 years	3	73.5	97.5	91.7	90.1

[a]Lifetime estimates based on *WMO/UNEP*, 2007.

During DC3 research flights, all canisters were pressurized to 35–40 psig. Sample collection time ranged from 0.5 to 1.5 min depending on altitude, and sample frequency ranged from every 0.5 – 5 min, depending on aircraft location relative to points of interest. An on-board live feed provided aircraft location, precipitation radar, wind direction, as well as mixing ratios of nitric oxide (NO), CO, and O_3. On a typical 5–8 h research flight, 70–110 samples were collected. All samples were shipped back to UC Irvine and analyzed by gas chromatography (GC) within 1 week of collection.

Previously designed and constructed analytical systems in the Rowland/Blake laboratory were used for VOC analysis. A brief description is provided below, and readers are referred to *Colman et al.* [2001] and *Simpson et al.* [2010] for a more in-depth description. VOC analysis was performed using HP 6890 gas chromatographs with a variety of column/detector combinations. Briefly, 2033 cm^3 sample aliquots were cryogenically pre-concentrated to remove volatile components (e.g., N_2, O_2, and Ar), then re-volatilized using a hot water bath. Samples were injected using a helium carrier gas and split into five different column/detector combinations. Two electron capture detectors (ECDs) were used to measure halocarbons and alkyl nitrates. Two Flame Ionization Detectors were used to measure C_2–C_{10} hydrocarbons, and a quadrupole mass spectrometer was used to measure selected halocarbons, hydrocarbons, and oxygenates. A standard is run after every eighth analysis, and the measured value of each compound in each standard is fit to a polynomial curve vs. sample injection time. All samples are normalized to these curves to adjust for any possible instrument drift over time. A total of 67 compounds were measured during DC3.

Mixing ratios of CO, N_2O, O_3, methane (CH_4), and water vapor were used throughout the data analysis process. CO, N_2O, and CH_4 were measured every 1 s by mid-infrared tunable diode laser absorption spectroscopy (DACOM), operated by NASA Langley [*Sachse and Hill*, 1987; *Sachse et al.*, 1991; *Diskin et al.*, 2002]. Water vapor was measured every 1 s by a near-infrared laser hygrometer, also operated by NASA Langley [*Diskin et al.*, 2002; *Podolske*, 2003]. O_3 was measured every 1 s using chemiluminescence, operated by NOAA's Earth System Research Laboratory [*Carroll et al.*, 1992]. These 1 s data were used to identify the exact times the DC-8 entered or exited a specific air mass—for example locating the exact times when the DC-8 entered and exited convective outflow. For correlation and direct use with WAS data, these 1 s data were averaged over the filling period of a given WAS canister (the so-called "WAS data merge," accessible at http://www-air.larc.nasa.gov/cgi-bin/ArcView/dc3). O_3 lidar profiles were also used to ascertain locations and shapes of potential stratospheric intrusions and were collected by a differential absorption lidar (DIAL) instrument, operated by NASA Langley [*Browell*, 1989; *Fenn et al.*, 1999].

Tropopause height was also calculated along the DC-8 flight path for each flight. Briefly, this was done by interpolating the National Centers for Environmental Prediction Global Forecast System model analysis (NCEP-GFS) in space and time and comparing to aircraft data. From this, both the local thermal and dynamic tropopause heights were calculated using the World Meteorological Organization (WMO) tropopause definition [*WMO*, 1957]. The associated uncertainty in calculated tropopause heights is proportional to the GFS vertical resolution, and is generally around ~500 m [*Homeyer et al.*, 2014]. These data are also available in the DC3 data merges, the link to which is provided in the previous paragraph.

3. Data Analysis

3.1. Development of a New Tracer for Stratospheric Air

To determine which air masses had stratospheric influence, a tracer that has a distinct tropospheric vs. stratospheric profile must be used, ideally with little to no altitudinal variation within the troposphere. To accomplish this, an ensemble of long-lived halocarbons was used. These halocarbons are listed in Table 1.

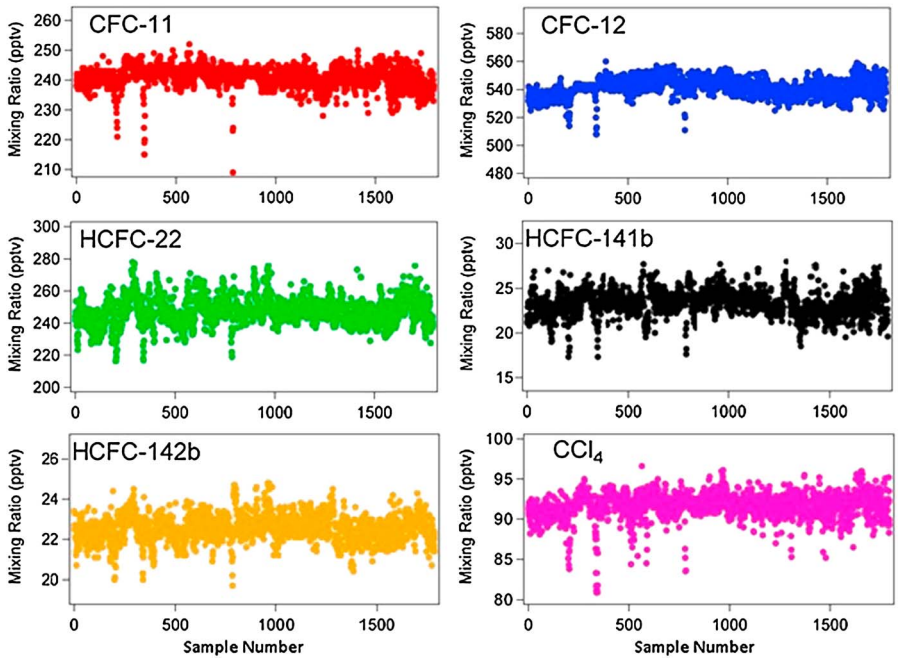

Figure 1. Long-lived halocarbons used as tracers for stratospheric air. Sample numbers are arranged in the chronological order in which they were collected during Deep Convection, Clouds, and Chemistry (DC3). Values below background mixing ratios are indicative of stratospheric influence in a sample.

These long-lived halocarbons are essentially inert with respect to gas-phase oxidation by OH. The only appreciable sink for these compounds is by UV photolysis, which is negligible in the troposphere. Furthermore, all six have sufficiently long atmospheric lifetimes that they are globally well mixed and have very little variation in tropospheric mixing ratios. CFC-11 and CFC-12 are listed as Class I ozone-depleting substances (ODS) by the US EPA, and their use in the US has been phased out under the Montreal Protocol and Clean Air Act [*EPA*, 2012]. As a result, tropospheric mixing ratios of CFC-11 and CFC-12 are essentially steady across the US [*Brown et al*., 2011; *Minschwaner et al*., 2013]. HCFC-22, HCFC-141b, and HCFC-142b are listed as Class II ODS. Their use is being phased out and is currently limited by caps set under the Clean Air Act, resulting in stable mixing ratios except when close to their limited sources [*Brown et al*., 2011]. Carbon tetrachloride is listed as a Class IV ODS, and its production has been restricted to limited industrial uses, also resulting in a stable tropospheric level [*Brown et al*., 2011]. In the stratosphere these compounds are exposed to a higher intensity of UV radiation, thereby accelerating their degradation relative to the troposphere [*WMO/UNEP*, 2007]. If a stratospheric air mass were to cross the tropopause, it would be distinguishable from background tropospheric air by a measurable reduction in the mixing ratios of these compounds. Qualitatively, this is evidenced by the simultaneous decrease in the mixing ratios of all six halocarbons used in this analysis, shown in Figure 1.

A simple quantitative analysis was used to differentiate "stratospherically influenced" (abbreviated SI throughout the rest of this paper) samples from tropospheric samples. In this case, SI samples could be samples collected in the stratosphere, in fresh stratospheric intrusions in the troposphere, or in air masses where a detectable amount of stratospheric air has mixed with tropospheric air. To be labeled as an SI sample, certain criteria had to be met: If, in a given sample, the mixing ratios of at least five of the six gases listed in Table 1 were in their respective lowest quartile from the entire DC3 data set, that sample was labeled as "SI." Of the 1795 whole air samples collected during DC3, only 96 met these criteria. These samples were collected on 13 of the 18 research flights, which are listed in Table 2.

3.2. Quality Control

To assess the sensitivity of this result to the criteria selected (that is, the number of SI samples detected by the method described above), the percentile used as a cutoff was allowed to vary. For example, if, instead of requiring at least five gases to have mixing ratios in their lowest 25%, we require at least five gases to

Table 2. Flights in Which Stratospherically Influenced (SI) Samples Were Collected

Research Flight	Date, Takeoff Time (UTC)	Primary Objective of Flight	Number of SI Samples Collected
1	5/18, 19:04	Active convection	18
2	5/19, 16:03	Active convection	17
3	5/21, 16:00	Active convection	12
4	5/25, 20:11	Active convection	3
5	5/26, 19:04	Tracking aged outflow	4
6	5/29, 19:54	Active convection	3
7	5/30, 18:33	Tracking aged outflow	7
11	6/6, 18:11	Active convection	2
13	6/11, 16:03	Active convection	5
14	6/15, 18:32	Active convection	6
15	6/16, 20:07	Active convection	3
16	6/17, 19:07	Tracking aged outflow	8
18	6/22, 19:54	Active convection, biomass burning	8

have mixing ratios in their lowest 30%, 194 SI samples are identified. Following this method, the cutoff percentile was allowed to vary by steps of 5% over the range of 10–50%, and the number of SI samples identified at each step was counted. These results are shown in Figure 2 and suggest that using 25% as a cutoff was the best way to maximize the number of SI samples identified while still remaining fairly conservative—using a cutoff larger than 25% leads to a marked increase in the number of SI samples identified and in the slope of each line segment.

Instrumental drift during the sample analysis stage could potentially produce a false-positive, as a low bias could be applied across all measured compounds in a given sample. To check for this, N_2O, which was measured by another instrument aboard the DC-8 (DOAS-DACOM), was used. Like the gases used in Table 1, N_2O also has a primary sink of UV photolysis in the stratosphere and can be used to identify some stratospheric air masses [*Ishijima et al.*, 2010; *Assonov et al.*, 2013]. Due to instrumental errors, N_2O measurements were not collected for flights 1, 6, and 13–18, and thus N_2O could not be used as a tracer alongside the gases listed in Table 1. However, of the SI samples where N_2O data are available, 84% have an N_2O mixing ratio in its lowest quartile from among all DC3 measurements. It should be noted that the average N_2O mixing ratio ($\pm 1\sigma$) from the DC3 WAS merge was 325.3 ± 1.7 pptv, while the lowest quartile threshold was 325.2 pptv.

4. Results

4.1. Spatial Distribution of Samples With Stratospheric Influence

During DC3, active convective storms were only sampled in three regions where ground imaging was available (section 2). As a result, sample locations were biased toward these three regions, and this bias is also reflected in the geographic distribution of SI samples, as seen in Figure 3. Of the 96 SI samples, 50 were collected in the first three research flights, and the majority of low-altitude SI samples were collected near the CO/WY/NE border. These trends were expected, as previous modeling and field work suggest that STT over the US peaks in winter and grows weaker into summer, with most deep STT events occurring over the western US [*Stohl et al.*, 2003; *Lefohn et al.*, 2011; *Kuang et al.*, 2012; *Langford et al.*, 2012; *Lin et al.*, 2012].

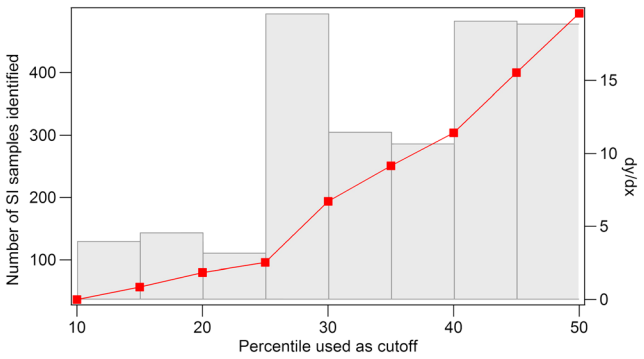

Figure 2. Variance in the number of stratospherically influenced (SI) samples identified by chosen cutoff percentiles (red squares). The slope of each line segment was calculated and is plotted as gray bars.

4.2. O_3 in SI Samples

To further test the effectiveness of using a composite of halocarbons as tracers of stratospheric air, a comparison with O_3, a more commonly used stratospheric tracer, was performed. To do this, samples with no stratospheric influence were

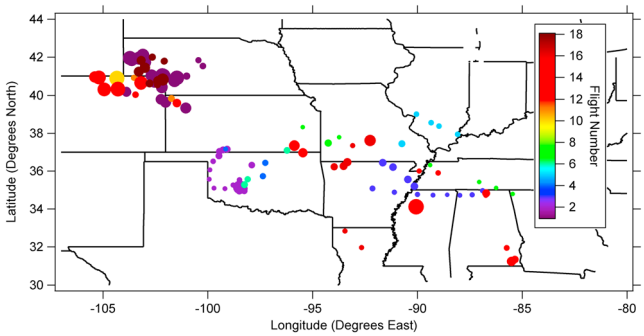

Figure 3. Location of whole air sampler (WAS) samples determined to have stratospheric influence. Samples are colorized by flight number, and sized by altitude with the largest dots being closest to ground level. Sample altitudes ranged from 0.8 to 12.5 km. The three primary areas of study are circled.

identified as those with no tracers from Table 1 having mixing ratios in their lowest quartile. O_3 values in these "non-SI" samples were fit to a line using a least squares linear regression (with altitude as the independent variable), and the 95% confidence interval for this line was calculated. It is important to note that, in this analysis, "non-SI" samples could include both polluted and non-polluted tropospheric air and therefore represents the regional troposphere as a whole rather than a true "background." At each altitude in which an SI sample was collected, the percent enhancement of O_3 (that is, enhancement in O_3 in SI samples relative to the modeled tropospheric O_3 "background") was calculated. Figure 4 shows the percent enhancement of O_3 for each SI sample. As expected, O_3 enhancements are largest at high altitudes where the DC-8 would have flown through fresh, undiluted stratospheric intrusions, or in the stratosphere itself. At low altitudes, modest enhancements were still observed. For example, our lowest-altitude SI sample (819 m above ground level) had an O_3 mixing ratio of 70 ppbv, an enhancement of $29 \pm 11\%$ over modeled tropospheric levels. This falls within the range observed by Langford (2012)—who observed a 23% O_3 enhancement at surface sites in southern California during a deep stratospheric intrusion—and Lin (2012) who observed surface O_3 levels of 60–75 ppbv across the western US during deep stratospheric intrusions. This sample, however, shows significant tropospheric character as evidenced by its CO mixing ratio of 130 ppbv. In fact, the majority of SI samples with modest O_3 enhancements ($<$30% above background) have CO mixing ratios over 100 ppbv.

A plot of O_3 vs CO for the WAS data merge shows two distinct branches: a positive slope indicating photochemical production of O_3 (that is, a tropospheric origin), and a negative slope indicating stratospheric origin (Figure 5). The area where these two lines intersect may be the result of mixing between tropospheric and stratospheric air. Here, we see that this mixing occurs at many altitudes—both near and well below the tropopause. *Pan* [2004] showed that the extratropical tropopause is best represented as a layer, rather than a surface. This layer can be as much as 3 km thick and is centered on the thermal tropopause. In this work, we use the thermal tropopause as the upper boundary of the troposphere. When our SI samples are highlighted in this tracer space (red dots in Figure 5), we see that some samples that are well within the tropospheric branch have stratospheric influence. These SI samples would go un-detected by conventional analysis, as O_3 has either been significantly diluted or chemically removed, and polluted air has masked the pristine stratospheric nature. However, these well-mixed samples may be important from a local chemistry standpoint, as described earlier in this work.

In the lower troposphere, this mixing likely occurred when deep stratospheric intrusions mixed with polluted air in the PBL, as has been described elsewhere [*Langford et al.*, 2012; *Lin et al.*, 2012]. In the upper troposphere, this mixing likely occurred when polluted air was lofted to the UT by deep convection in the vicinity of a stratospheric intrusion. In the following sections, we focus our attention on this mixing in the UT and aim to do the following: show evidence of a specific case where polluted convective outflow mixed with stratospheric air, determine a timescale for this mixing during DC3 (did it occur while storms were active, or after they had dissipated?), and assess the extent of this mixing during DC3 and potential impacts on chemistry of the UT.

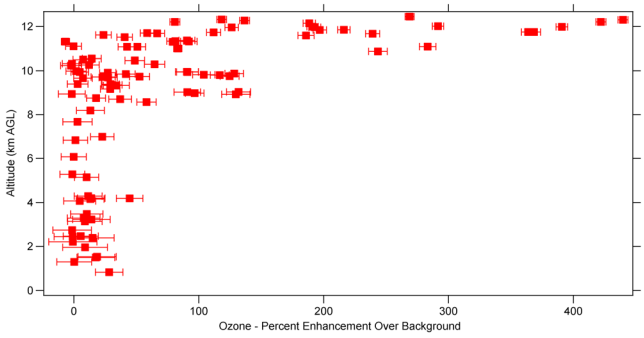

Figure 4. Percent enhancement of O_3 in SI samples compared to the modeled background.

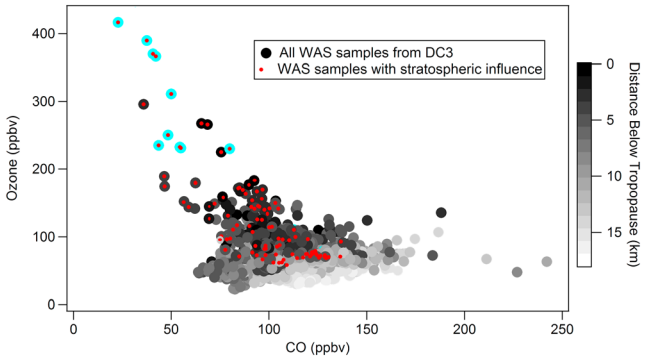

Figure 5. O_3 vs carbon monoxide (CO) for the WAS data merge. Samples that met the criteria to be labeled as SI samples are indicated by red dots. All samples are colored by distance below the thermal tropopause, and cyan samples were collected above the thermal tropopause.

4.3. Case Study: Evidence of Stratospheric Air Mixing With Aged, Polluted Convective Outflow

To determine whether or not a specific air mass has been impacted by convective lofting of anthropogenically influenced air, a filter must be applied. An ideal tracer with which to create this filter must have the following characteristics: (1) a significant source that is associated with human activity, (2) widespread use over the entire DC3 study region, and (3) a moderate atmospheric lifetime (long enough so we can detect both fresh pollution and pollution that is a few days old, but short enough to still have a strong vertical gradient). CO (lifetime ~ 2 months) is a useful marker for anthropogenic activity, but its long lifetime leads to an observable seasonal trend even in background UT air, and thus it is not necessarily a good marker of individual convective events [*González Abad et al.*, 2011; *Huang et al.*, 2012]. Throughout the DC3 study region, persistent enhancements in light hydrocarbons have been observed, due to regional urban emissions and extensive oil and gas collection and processing throughout the Great Plains and Colorado [*Trainer et al.*, 1995; *Katzenstein et al.*, 2003; *Baker et al.*, 2008; *Pétron et al.*, 2012; *Gilman et al.*, 2013]. Of these light hydrocarbons, propane and *n*-butane are good choices for anthropogenic filters. With average atmospheric lifetimes of ~11 days and ~5 days respectively, enhancements in propane and *n*-butane mixing ratios will be measured even several days downwind of sources, leading to widespread enhancement over the entire study region of DC3, while, in the absence of convection, these gases have very low mixing ratios in the UT. In fact, from all DC3 WAS samples collected below an altitude of 2 km, the lowest measured *n*-butane and propane mixing ratios were 50 pptv and 205 pptv, respectively, while in the UT, background propane values were regularly measured below 205 pptv and background *n*-butane values were regularly measured below 50 pptv. For reference, the average propane and n-butane mixing ratios encountered below altitudes of 2 km during DC3 were 2268 pptv and 880 pptv, respectively. Thus, if a deep convective storm were to occur anywhere over the DC3 study region, air from the PBL with propane values greater than 205 pptv and *n*-butane values greater than 50 pptv would be lofted to the UT, and a strong enhancement in both propane and *n*-butane would be observed in association with elevated levels of water vapor. This is shown in Figure 6, where, at a given altitude in the UT, high propane and *n*-butane levels are always associated with high levels of water vapor, indicating recent vertical transport associated with deep convection [*Aschmann et al.*, 2009; *Bechara et al.*, 2010]. For comparison, CO is also shown in Figure 6, and many high-altitude samples with low levels of water vapor are shown to have relatively high values of CO (over 125 ppbv in some cases). This indicates that enhanced CO values can be present in the UT without association to recent convection. For reference, the lowest CO value measured below 2 km was 89 ppbv, and the average CO mixing ratio from all samples collected below 2 km was 125 ppbv. Thus, a filter was constructed whereby samples with both a propane mixing ratio exceeding 205 pptv and an *n*-butane mixing ratio exceeding 50 pptv were labeled as anthropogenically influenced. Sensitivity tests show that decreasing these requirements (for example, using 160 pptv of propane and 40 pptv of *n*-butane as cutoffs) results in a large increase in the number of anthropogenically influence samples detected, while increasing these requirements results in a small increase in the number of anthropogenically influence samples detected. In essence, nearly all anthropogenically influenced samples have propane mixing ratios much greater than 205 pptv and *n*-butane mixing ratios much greater than 50 pptv.

During DC3 research flight 16 (17 June 2012), the DC-8 had a primary objective of tracking down and probing aged outflow from a storm that had occurred the previous day over Oklahoma. The DC-8 altitude profile for this flight is shown in Figure 7. While flying at altitudes between 8 and 12 km over the target area, the DC-8 regularly encountered air with elevated propane and *n*-butane values (i.e., over 205 pptv and 50 pptv, respectively), indicative of convective outflow. In Figure 7, propane mixing ratios are indicated by red bars, while *n*-butane mixing ratios are omitted for the sake of clarity. At 21:00 and 21:30 UTC air with elevated

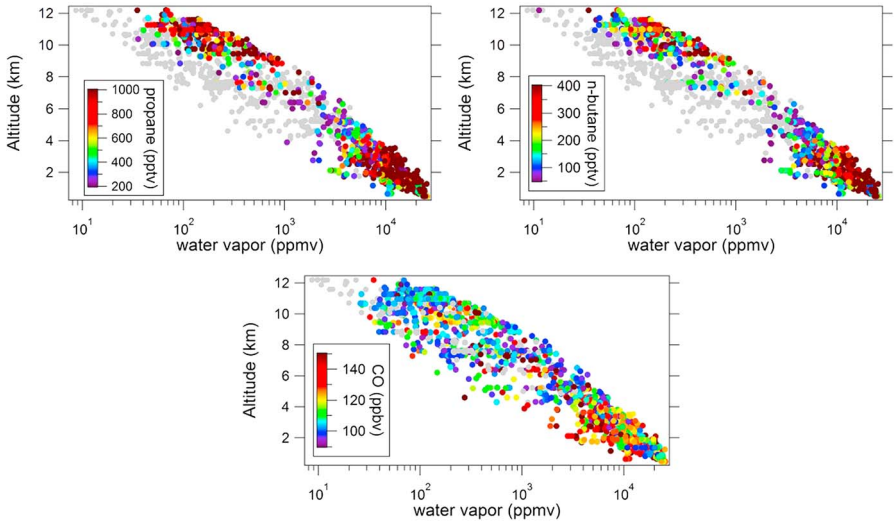

Figure 6. Altitude profiles of water vapor from the DC3 WAS data merge. On the upper left panel, samples are colored by propane values, where values below 205 pptv are colored gray. On the upper right panel, samples are colored by *n*-butane values, where values below 50 pptv are colored gray. On the bottom panel, samples are colored by CO values, where values below 90 ppb are colored gray.

propane and O_3 levels was encountered. In these patches of high O_3, four SI samples were identified. The entire flight took place below the thermal tropopause, suggesting that at some point in the previous 24 h, stratospheric air had entered the troposphere and mixed with this outflow.

To determine when this mixing took place, we looked at the origin of this convective outflow. Back trajectory analyses were performed using the NOAA HYSPLIT model. Although these trajectories do not accurately reproduce convective motion, they do identify the location of convective systems responsible for the observed outflow. These analyses show that the aged convective outflow sampled during research flight 16 originated from a convective storm near the Texas/Oklahoma border that had occurred the previous day (research flight 15; 16 June 2012). During research flight 15, the DC-8 sampled the inflow and outflow regions of this storm. The inflow air contained high levels of propane, *n*-butane, and other hydrocarbons associated with the widespread regional oil and natural gas extraction activities. While sampling the outflow from the active storm on 16 June, three SI samples were detected at altitudes of 11–11.5 km. Of these three SI samples, two had evidence of mixing with polluted convective outflow—elevated levels of not only propane and *n*-butane, but other short-lived hydrocarbons associated with oil and natural gas extraction including *n*-heptane (lifetime ~ 1.7 days) and ethene (lifetime ~ 1.4 days). This supports a hypothesis that mixing with stratospheric air may occur as a convective storm is developing. However, since only three SI samples were collected during research flight 15, it is difficult to draw any firm conclusions about the dynamics of mixing near an active storm. For a more detailed perspective on the dynamics of this mixing, we examined a flight where a higher number of SI samples were collected near an active storm.

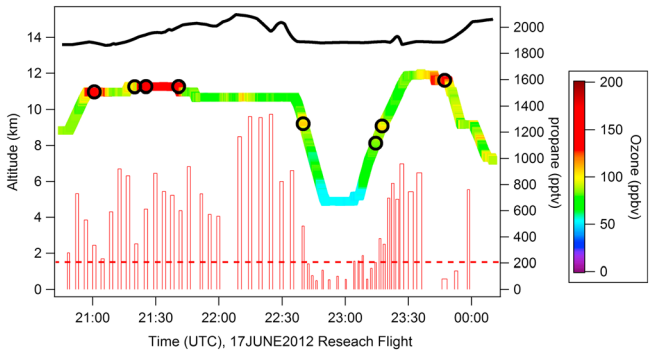

Figure 7. The DC-8 altitude profile for DC3 research flight 16. The flight path is colored by 1 s O_3 measurements, and SI samples are marked with circles. WAS propane mixing ratios (right axis) are shown as red bars and are used to indicate the presence of convective outflow. A dashed red line marks the propane cutoff value of 205 pptv described in section 4.3. The entire flight took place below the thermal tropopause, which is indicated by a thick black line.

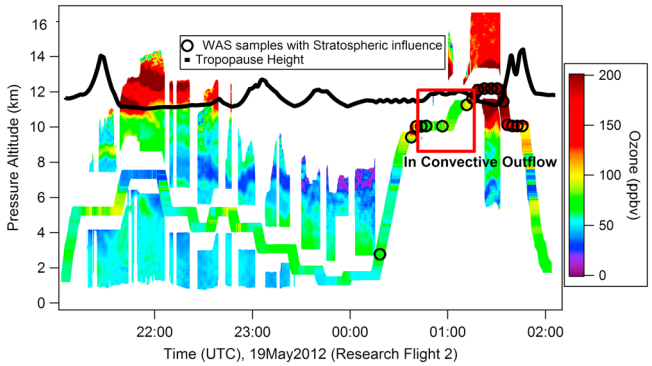

Figure 8. The DC-8 altitude profile for DC3 research flight 2. The altitude profile (flight track) is colored by 1 s O_3 measurements, and SI samples are indicated by circles. The DC-8 also carried an O_3 lidar, the profile of which is shown above and below the altitude profile and colorized on the same scale. The thermal tropopause is represented as a thick black line. The period when the DC-8 passed through the outflow region of the storm is indicated by a red rectangle.

4.4. Case Study: Evidence of Stratospheric Air Mixing With Outflow From an Active Storm

To more thoroughly evaluate the mixing dynamics near active storms, more SI samples are needed in the vicinity of a storm. Research flight 2 (19 May 2012) had a primary objective of probing the inflow and outflow regions of an isolated, active convective storm over Oklahoma. During this flight, 17 SI samples were collected. The DC-8 flew L-shaped patterns in the low-altitude inflow region of the storm—which was characterized by elevated levels of hydrocarbons and biogenic emissions like isoprene, and stable levels of the halocarbons listed in Table 1—then spiraled up to an altitude of 12 km to probe the outflow of this storm. The altitude profile for this flight is shown in Figure 8. The track of the spiral-up and outflow pass segments are shown in Figure 9.

Before entering the convective outflow (end of the upward spiral segment), an air mass with strong stratospheric character was observed (O_3 levels above 100 ppbv, large decreases in mixing ratios of long-lived halocarbons and N_2O, low water vapor content, very low levels of hydrocarbons), and three SI samples were identified. These SI samples were located about 1.3 km below the thermal tropopause. Then, from 00:43 to 01:16 UTC the DC-8 flew two passes through convective outflow from this active storm (red rectangle in Figure 8; red oval in Figure 9). During both of these outflow passes, the DC-8 remained below the thermal tropopause. The outflow was marked by large enhancements in both short-lived and long-lived hydrocarbons. For example, long-lived species like ethane (lifetime ~ 47 days) were enhanced by several hundred percent over background UT mixing ratios at the same time that very-short-lived species (like isoprene, which has an average atmospheric lifetime of ~ 3 h and is below our 3 pptv detection limit in background UT air masses) were observed in detectable amounts. Upon entering the convective outflow, O_3 levels decreased, water vapor increased, and hydrocarbon levels increased, effectively masking any obvious stratospheric character that may be mixed in. However, four SI samples were identified in the outflow, indicating that stratospheric air had indeed mixed with the outflow.

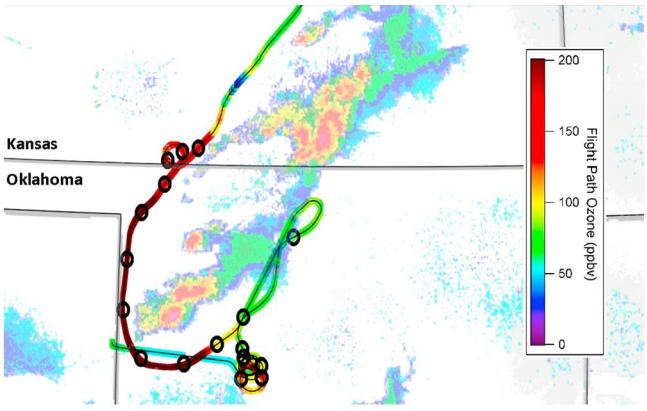

Figure 9. The DC-8 flight track for the spiral-up and outflow segments of DC3 research flight 2 (flight path begins at 23:55 UTC in the bottom left corner, and ends at 02:00 UTC at the top of the image). The flight path is colorized by 1 s O_3 measurements, and SI samples are indicated by black circles. A NEXRAD radar image from 01:05 UTC is overlain, showing the weather pattern probed by the DC-8. The portion of the flight where the DC-8 flew through convective outflow is circled in red.

After leaving the convective outflow, the DC-8 ascended to 12 km, flew around the south end of the convective cell, and returned to Salina along the backside of the storm front. Upon ascending, the DC-8 briefly crossed the thermal tropopause and sampled stratospheric air around 01:20 UTC. Four SI samples were collected during this flight segment. After spending several minutes above the tropopause, the DC-8 then descended below the

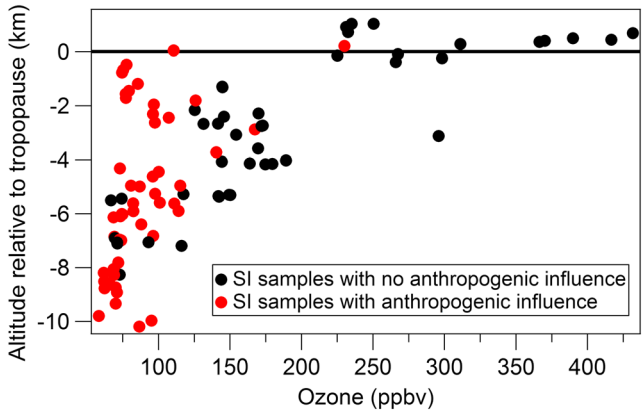

Figure 10. All SI samples from DC3. Black circles indicate samples that did not meet our criteria to be labeled "anthropogenically influenced", and red circles indicate samples that did meet these criteria. Altitudes are listed relative to the tropopause height calculated for each sample, where positive altitudes were collected above the tropopause and negative altitudes were collected below the tropopause.

tropopause, but the same strong stratospheric character remained, and five SI samples were identified. Lidar O_3 profiles from this backside segment show an air mass with a strong stratospheric character reaching down to 10 km (Figure 8). A dip in the thermal tropopause height, from 12 to 11 km, was also observed in this region. From this, it is apparent that stratospheric air had penetrated below the tropopause on the backside of the storm front, and this stratospheric air had mixed, in varying degrees, with the outflow on the east side of the storm. This information, combined with the in situ evidence regarding the SI samples, shows that the polluted boundary layer air encountered here was rapidly mixed with stratospheric air upon being lofted to the UT. In this case, mixing was likely facilitated by the strong northwesterly winds observed in the UT behind the storm front.

4.5. Evidence of Wide-Scale Mixing of Stratospheric Air With Convective Outflow

To assess the overall impact of mixing between polluted convective outflow and stratospheric air, the propane and *n*-butane filter described in section 4.3 was applied to all SI samples. O_3 was used as an approximate indicator for the level of dilution of a stratospheric air mass. SI samples with high O_3 values were either collected in the stratosphere or were fresh, recent stratospheric intrusions. SI samples with reduced O_3 values (i.e., below 150 ppbv) are the result of dilution of a stratospheric air mass—either by mixing with clean background air in the FT, mixing with boundary layer air that has been convectively lofted into the FT, or direct mixing with boundary layer air during a deep stratospheric intrusion. It should be noted that O_3 levels are not constant within the stratosphere and are subject to variation by altitude, geographic location, and seasonal changes [*Stohl et al.*, 2003; *Zeng et al.*, 2010]. Because of this, we make no attempt to quantify the amount of dilution observed here.

Figure 10 shows the tropopause-relative altitude profile for O_3 in all SI samples collected during DC3. Based on their propane and *n*-butane mixing ratios, samples were binned as having relatively recent anthropogenic influence (propane $>$ 205 pptv, *n*-butane $>$ 50 pptv) or not. As expected, SI samples with the highest O_3 values are located near the tropopause and show no recent anthropogenic influence, as they consist mostly of undiluted stratospheric air. By contrast, most SI samples collected below the tropopause had elevated propane and *n*-butane levels, implying that the SI samples had mixed with polluted boundary layer air to some extent. Based on all SI samples with O_3 values below 150 ppbv, 72% met our criteria to be labeled as anthropogenically influenced. Even in the UT, most SI samples that have experienced significant mixing with tropospheric air ($O_3 < 150$ ppbv) have done so by mixing with polluted air rather than clean free tropospheric air. This result suggests that over central US in late spring the primary mixing mechanism for storm-associated stratospheric intrusions is the mixing with convective outflow that has recently been lifted out of the polluted boundary layer.

4.6. Effects on OH Production

With moist air from convective outflow mixing with the high-O_3 air of a stratospheric intrusion, the oxidizing capacity of convective outflow—and the regional upper troposphere—may be altered via an increased production of OH radicals. When comparing the relative OH productivity of two air masses, equation (5) can be further simplified under the assumption that both air masses have identical temperature and pressure conditions:

$$\frac{\mathbf{P_{OH,1}}}{\mathbf{P_{OH,2}}} = \frac{[\mathbf{H_2O}]_1[\mathbf{O_3}]_1}{[\mathbf{H_2O}]_2[\mathbf{O_3}]_2} \quad (6)$$

Table 3 shows relevant chemical data used for calculating this ratio and includes the mean and 95% confidence interval for both H_2O and O_3. SI samples collected at altitudes above 8 km with O_3 values above 200 ppbv and

Table 3. Chemical Data for Different Air Masses in the Upper Troposphere (UT) and Their Calculated Instantaneous Hydroxyl Radical (OH) Production[a]

Air Mass	Water (H_2O) (ppb)	Ozone (O_3) (ppb)	$\frac{P_{OH,mixed}}{P_{OH,air\ \ mass}}$
Fresh stratospheric intrusion	13,000 ± 8300	333 ± 128	11 ± 8
Background UT	138,000 ± 39,000	82 ± 18	4.2 ± 1.8
Mixed stratospheric/convective outflow	371,000 ± 64,080	125 ± 50	1

[a]Here, "mixed" refers to air masses where stratospheric air has mixed with convective outflow.

no anthropogenic influence (as per the filter described in section 4.3) were labeled as fresh stratospheric intrusions. Background UT samples were identified as WAS samples collected above 8 km where none of the tracers from Table 1 were at levels in their lowest quartile and no anthropogenic influence was detected by our filter (and therefore, over this study region, little-to-no convective influence, either). Mixed stratospheric/convective outflow samples were identified as SI samples collected above 8 km with detectable anthropogenic influence.

Using equation (6), P_{OH} for mixed stratospheric/convective outflow was calculated to be higher than P_{OH} for fresh stratospheric intrusions by a factor of 11 ± 8. The high uncertainty is due to the low levels of water vapor present in stratospheric air and the wide range of O_3 values allowed to be classified as "fresh stratospheric intrusions"—a difference of even a few ppb of O_3 and water vapor between samples results in a high uncertainty in the mean value. Comparing mixed stratospheric/convective outflow to background UT air, this factor was calculated to be 4.2 ± 1.8. These results are summarized in Table 3.

Chemical loss of OH (L_{OH}) is also expected to be different between these air masses, and must be accounted for to fully understand the net change in OH (equation (7)):

$$\frac{d\mathbf{OH}}{d\mathbf{t}} = \mathbf{P_{OH}} - \mathbf{L_{OH}} \tag{7}$$

L_{OH} can be estimated by calculating OH reactivity (k_{OH}) using equation (8):

$$\mathbf{L_{OH}} \approx \mathbf{k_{OH}} = \sum \mathbf{k_i}[\mathbf{trace\ gas}]_\mathbf{i} \tag{8}$$

In this equation, k_i represents the rate constant for the reaction of trace gas *i* with OH, where trace gases include all VOCs measured, as well as CO and methane (CH_4). In all of air masses presented in Table 3, CO and CH_4 were found to contribute to more than 85% of the total OH reactivity. This is an important result, because the variation in CO and CH_4 between air masses is significantly less than the variation between VOCs. For example, relative to clean background UT air or fresh stratospheric intrusions, mixed stratospheric/convective outflow air masses may have VOC enhancements in excess of 100%, while both CO and CH_4 were typically enhanced by ~25% and 2%, respectively. This means that, despite large enhancements in VOC mixing ratios, L_{OH} in mixed stratospheric/convective outflow is estimated to be higher than L_{OH} in background UT air and fresh stratospheric intrusions by a factor of 1.5, at most. In comparison to P_{OH}, which was significantly enhanced in mixed stratospheric/convective outflow airmasses (see Table 3), the enhancement in L_{OH} is small enough to make little difference in the net production of OH. Thus, we expect mixing between stratospheric air and convective outflow to produce a net gain in OH in the UT.

If our hypothesis from section 4.5 is true—that storm-associated stratospheric intrusions often mix with convective outflow—then this could be a potentially large source of OH radicals in the UT over the central US and affect chemistry in the UT, particularly in areas where deep convection is frequent. In the presence of this type of mixing, the lifetimes of OH-controlled VOCs would be shorter than currently predicted. This could alter the radiative forcing of the UT by reducing the lifetimes of radiatively important gases like CH_4 and ethane, while cirrus cloud formation may be altered due to the enhanced production of secondary VOCs and their associated changes in gas/particle partitioning [*Riese et al.*, 2012]. At this point, however, we cannot say how frequent these mixing events are, nor can we say with certainty that these results hold true on a global scale over a period of a whole year. Further work must be done to assess the validity of this study.

5. Conclusions

Using a suite of long-lived halocarbons as a tracer, stratospherically influenced air was detected throughout the DC3 study region. O_3 levels in these SI samples indicated that, below the tropopause, stratospheric air had

been mixed with tropospheric air on a number of occasions. Many of these samples with mixed stratospheric-tropospheric character had elevated levels of CO—indicative of anthropogenic influence. These mixed samples were identified in both the PBL and the UT. During DC3, rapid vertical transport of polluted air occurred via deep convective lofting of air from the PBL to the UT. This polluted convective outflow was detected during active storms, where it remained in the UT and was transported downwind for several days. To investigate the process by which stratospheric air mixes with convectively lofted polluted air, a case study was performed: using two hydrocarbons with moderate lifetimes (*n*-butane and propane) and back trajectories, aged, polluted convective outflow (lofted to the UT one day prior to sampling) was identified as having been sampled during research flight 16. Embedded within this outflow were six samples that had both anthropogenic and stratospheric influence. A case study performed on a flight where an active storm was sampled (research flight 2) also shows evidence of this type of mixing. During this flight, a large stratospheric intrusion was identified behind a storm front passing over Oklahoma. While probing the outflow from this storm, five samples were collected that met our criteria to be labeled as stratospherically influenced. These results indicate that active convection may act to facilitate the mixing between stratospheric and polluted air in the UT, although we do not attempt to draw any conclusions about the meteorological relationship between colocated stratospheric intrusions and deep convective storms and the frequency by which this type of mixing occurs. Since the DC-8 primarily sampled convective outflow below the tropopause, and nearly all SI samples with detectable anthropogenic influence were collected below the tropopause, we can not speculate about the presence of this type of mixing in the lowermost stratosphere.

Of all SI samples collected during DC3, 72% showed detectable anthropogenic influence. In the UT, the majority of SI samples that had experienced some degree of mixing with tropospheric air had done so by mixing with polluted convective outflow. Relative to tropospheric air, stratospheric air has very high O_3 levels, while, relative to stratospheric air, tropospheric air has very high levels of water vapor. Thus, mixing between the two is expected to lead to an enhanced instantaneous production of OH relative to un-mixed stratospheric or tropospheric air. Indeed, based on O_3 and water vapor mixing ratios measured during DC3, air masses that had both stratospheric and anthropogenic influence was calculated to have an instantaneous production of OH that is 11 ± 8 times higher than undiluted stratospheric intrusions, and 4.2 ± 1.8 times higher than background tropospheric air. This process creates a unique chemical environment where boundary layer pollution that is convectively lofted in the upper troposphere may experience higher-than-expected loss rates of OH-controlled trace gases. Although the work presented here may help lay the groundwork for understanding this type of mixing, future measurements and modeling studies must be done to assess the regional, global, and temporal trends of this type of mixing, and any potential impacts on tropospheric chemistry.

Acknowledgments

Data used in this paper can be accessed via the NASA Airborne Science Data for Atmospheric Composition website (http://www-air.larc.nasa.gov/cgi-bin/ArcView/dc3). This work was supported by NASA grant NNX12AB76G. We would like to thank all members of the DC3 science and planning teams for their work and assistance in the field. We also thank our colleagues at UCI—Brent Love, Gloria Liu, Josette Marrero, Greg Hartt, Yu-Hsin Hung, Charlie Hirsch, and Aaron Gartner—for their assistance in the laboratory. We also thank Owen R. Cooper for providing useful comments and providing a creative spark during the early stages of this work, as well as our reviewers for providing many useful comments that helped make this a better paper.

References

Ancellet, G., and M. Beekmann (1994), Impact of a cutoff low development on downward transport of ozone in the troposphere, *J. Geophys. Res.*, *99*, 3451–3468, doi:10.1029/93JD02551.

Apel, E. C., et al. (2012), Impact of the deep convection of isoprene and other reactive trace species on radicals and ozone in the upper troposphere, *Atmos. Chem. Phys.*, *12*(2), 1135–1150, doi:10.5194/acp-12-1135-2012.

Aschmann, J., B. M. Sinnhuber, E. L. Atlas, and S. M. Schauffler (2009), Modeling the transport of very short-lived substances into the tropical upper troposphere and lower stratosphere, *Atmos. Chem. Phys.*, *9*(5), 18,511–18,543, doi:10.5194/acpd-9-18511-2009.

Assonov, S. S., C. A. M. Brenninkmeijer, T. Schuck, and T. Umezawa (2013), N_2O as a tracer of mixing stratospheric and tropospheric air based on CARIBIC data with applications for CO_2, *Atmos. Environ.*, *79*, 769–779, doi:10.1016/j.atmosenv.2013.07.035.

Avery, M., et al. (2010), Convective distribution of tropospheric ozone and tracers in the Central American ITCZ Region: Evidence from Observations During TC4, *J. Geophys. Res.*, *115*, D00J21, doi:10.1029/2009JD013450.

Baker, A. K., A. J. Beyersdorf, L. A. Doezema, A. Katzenstein, S. Meinardi, I. J. Simpson, D. R. Blake, and F. Sherwood Rowland (2008), Measurements of nonmethane hydrocarbons in 28 United States cities, *Atmos. Environ.*, *42*(1), 170–182, doi:10.1016/j.atmosenv.2007.09.007.

Bechara, J., A. Borbon, C. Jambert, A. Colomb, and P. E. Perros (2010), Evidence of the impact of deep convection on reactive Volatile Organic Compounds in the upper tropical troposphere during the AMMA experiment in West Africa, *Atmos. Chem. Phys.*, *10*(21), 10,321–10,334, doi:10.5194/acp-10-10321-2010.

Bithell, M., G. Vaughan, and L. Gray (2000), Persistence of stratospheric ozone layers in the troposphere, *Atmos. Environ.*, *34*(16), 2563–2570, doi:10.1016/S1352-2310(99)00497-5.

Browell, E. V. (1989), Differential absorption lidar sensing of ozone, *Proc. IEEE*, *77*(3), 419–432, doi:10.1109/5.24128.

Browell, E. V. (2003), Ozone, aerosol, potential vorticity, and trace gas trends observed at high-latitudes over North America from February to May 2000, *J. Geophys. Res.*, *108*(D4), 8369, doi:10.1029/2001JD001390.

Brown, A. T., M. P. Chipperfield, C. Boone, C. Wilson, K. A. Walker, and P. F. Bernath (2011), Trends in atmospheric halogen containing gases since 2004, *J. Quant. Spectros. Radiat. Transfer*, *112*(16), 2552–2566, doi:10.1016/j.jqsrt.2011.07.005.

Büker, M. L., M. H. Hitchman, G. J. Tripoli, R. B. Pierce, E. V. Browell, and J. A. Al-Saadi (2008), Long-range convective ozone transport during INTEX, *J. Geophys. Res.*, *113*, D14S90, doi:10.1029/2007JD009345.

Carbone, R. E., J. D. Tuttle, A. Ahijevych, and S. B. Trier (2002), Inferences of predictability associated with warm season precipitation episodes, *J. Atmos. Sci.*, *59*(13), 2033–2056, doi:10.1175/1520-0469.

Carroll, M. A., B. A. Ridley, D. D. Montzka, G. Hubler, J. G. Walega, and R. B. Norton (1992), Measurements of nitric oxide and nitrogen dioxide during the Mauna Loa observatory, *J. Geophys. Res.*, *97*, 10,361–10,374, doi:10.1029/91JD02296.

Cho, J. Y. N., R. E. Newell, B. Grant, C. F. Butler, and M. A. Fenn (2001), Observation of pollution plume capping by a tropopause fold measurement, *Geophys. Res. Lett.*, *28*, 3243–3246, doi:10.1029/2001GL012898.

Colette, A., and G. Ancellet (2006), Variability of the tropospheric mixing and of streamer formation and their impact on the lifetime of observed ozone layers, *Geophys. Res. Lett.*, *33*, L09808, doi:10.1029/2006GL025793.

Colman, J., A. Swanson, S. Meinardi, B. Sive, D. R. Blake, and F. S. Rowland (2001), Description of the analysis of a wide range of volatile organic compounds in whole air samples collected during PEM-Tropics A and B, *Anal. Chem.*, *73*, 3723–3731.

Crutzen, P., and P. Zimmerman (1991), The changing photochemistry of the troposphere, *Tellus A*, doi:10.3402/tellusa.v43i4.11943.

Crutzen, P. J., M. G. Lawrence, and U. Paeschl (1999), On the background photochemistry of tropospheric ozone, *Tellus A*, doi:10.3402/tellusa.v51i1.12310.

Dibb, J. E., L. D. Meeker, R. C. Finkel, J. R. Southon, M. W. Caffee, and L. A. Barrie (1994), Estimation of stratospheric input to the Arctic troposphere: 7Be and 10Be in aerosols at Alert, Canada, *J. Geophys. Res.*, *99*, 855–864, doi:10.1029/94JD00742.

Diskin, G. S., J. R. Podolske, G. W. Sachse, and T. A. Slate (2002), Open-path airborne tunable diode laser hygrometer, in *Proceedings of the Society for Photo-Optical Instrumentation Engineers (SPIE)*, vol. 4817, edited by A. Fried, pp. 196–204, Diode Lasers and Applications in Atmospheric Sensing, Seattle, Wash.

Doering, C., and R. Akber (2008), Beryllium-7 in near-surface air and deposition at Brisbane, Australia, *J. Environ. Radioact.*, *99*(3), 461–467, doi:10.1016/j.jenvrad.2007.08.017.

EPA (2012), Subchapter VI - Stratospheric ozone protection, *Clean Air Act Title VI*. [Available at http://epa.gov/oar/caa/title6.html.]

Fenn, A., et al. (1999), Ozone and Aerosol distributions and air mass characteristics over the South Pacific during the burning season, *J. Geophys. Res.*, *104*, 16,197–16,212, doi:10.1029/1999JD900065.

Fusco, A. C. (2003), Analysis of 1970–1995 trends in tropospheric ozone at Northern Hemisphere midlatitudes with the GEOS-CHEM model, *J. Geophys. Res.*, *108*(D15), 4449, doi:10.1029/2002JD002742.

Gerasopoulos, E., P. Zanis, A. Stohl, C. S. Zerefos, and C. Papastefanou (2001), A climatology of 7 Be at four high-altitude stations at the Alps and the Northern Apennines, *Atmos. Chem. Phys. Discuss.*, *35*, 6347–6360, doi:10.1016/S1352-2310(01)00400-9.

Gilman, J. B., B. M. Lerner, W. C. Kuster, and J. A. de Gouw (2013), Source signature of volatile organic compounds from oil and natural gas operations in northeastern Colorado, *Environ. Sci. Technol.*, *47*(3), 1297–1305, doi:10.1021/es304119a.

González Abad, G., et al. (2011), Ethane, ethyne and carbon monoxide concentrations in the upper troposphere and lower stratosphere from ACE and GEOS-Chem: A comparison study, *Atmos. Chem. Phys.*, *11*(18), 9927–9941, doi:10.5194/acp-11-9927-2011.

Hartmann, D. L., et al. (2013), Observations: Atmosphere and surface, in *Climate Change 2013: The Physical Science Basis. Contribution of Working Group I to the Fifth Assessment Report of the Intergovernmental Panel on Climate Change*, edited by G.-K. Stocker et al., Cambridge Univ. Press, Cambridge, U. K., and New York.

Homeyer, C. R., K. P. Bowman, L. L. Pan, M. A. Zondlo, and J. F. Bresch (2011), Convective injection into stratospheric intrusions, *J. Geophys. Res.*, *116*, D23304, doi:10.1029/2011JD016724.

Homeyer, C. R., et al. (2014), Convective transport of water vapor into the lower stratosphere observed during double tropopause events, *J. Geophys. Res. Atmos.*, doi:10.1002/2014JD021485.

Huang, L., R. Fu, J. H. Jiang, J. S. Wright, and M. Luo (2012), Geographic and seasonal distributions of CO transport pathways and their roles in determining CO centers in the upper troposphere, *Atmos. Chem. Phys.*, *12*(10), 4683–4698, doi:10.5194/acp-12-4683-2012.

Ishijima, K., et al. (2010), Stratospheric influence on the seasonal cycle of nitrous oxide in the troposphere as deduced from aircraft observations and model simulations, *J. Geophys. Res.*, *115*, D20308, doi:10.1029/2009JD013322.

Katzenstein, A. S., L. A. Doezema, I. J. Simpson, D. R. Blake, and F. S. Rowland (2003), Extensive regional atmospheric hydrocarbon pollution in the southwestern United States, *Proc. Natl. Acad. Sci. U.S.A.*, *100*(21), 11,975–11,979, doi:10.1073/pnas.1635258100.

Koch, D., and M. Mann (1996), Koch 1996 - Spatial and temporal variability of 7Be surface concentrations.pdf, *Tellus*, *48B*, 387–396.

Kuang, S., M. J. Newchurch, J. Burris, L. Wang, K. Knupp, and G. Huang (2012), Stratosphere-to-troposphere transport revealed by ground-based lidar and ozonesonde at a midlatitude site, *J. Geophys. Res.*, *117*, D18305, doi:10.1029/2012JD017695.

Langford, A. O., C. D. Masterst, M. H. Proffitt, E. Hsie, and A. F. Tuck (1996), Ozone measurements in a tropopause with a cut-off low system, *Geophys. Res. Lett.*, *23*, 2501–2504, doi:10.1029/96GL02227.

Langford, A. O., J. Brioude, O. R. Cooper, C. J. Senff, R. J. Alvarez, R. M. Hardesty, B. J. Johnson, and S. J. Oltmans (2012), Stratospheric influence on surface ozone in the Los Angeles area during late spring and early summer of 2010, *J. Geophys. Res.*, *117*, D00V06, doi:10.1029/2011JD016766.

Lefohn, A. S., H. Wernli, D. Shadwick, S. Limbach, S. J. Oltmans, and M. Shapiro (2011), The importance of stratospheric–tropospheric transport in affecting surface ozone concentrations in the western and northern tier of the United States, *Atmos. Environ.*, *45*(28), 4845–4857, doi:10.1016/j.atmosenv.2011.06.014.

Lin, M., A. M. Fiore, O. R. Cooper, L. W. Horowitz, A. O. Langford, H. Levy, B. J. Johnson, V. Naik, S. J. Oltmans, and C. J. Senff (2012), Springtime high surface ozone events over the western United States: Quantifying the role of stratospheric intrusions, *J. Geophys. Res.*, *117*, D00V22, doi:10.1029/2012JD018151.

Michelsen, H. J., R. J. Salawitch, P. O. Wennberg, and J. G. Anderson (1994), Production of O(1D) from Photolysis of O_3, *Geophys. Res. Lett.*, *21*, 2227–2230, doi:10.1029/94GL02052.

Minschwaner, K., L. Hoffmann, A. Brown, M. Riese, R. Müller, and P. F. Bernath (2013), Stratospheric loss and atmospheric lifetimes of CFC-11 and CFC-12 derived from satellite observations, *Atmos. Chem. Phys.*, *13*(8), 4253–4263, doi:10.5194/acp-13-4253-2013.

Pan, L. L. (2004), Definitions and sharpness of the extratropical tropopause: A trace gas perspective, *J. Geophys. Res.*, *109*, D23103, doi:10.1029/2004JD004982.

Pan, L., S. Honomichi, C. Homeyer, M. Barth, J. Hair, M. Fenn, C. Butler, G. Diskin, and H. Huntrieser (2014), Private Communication.

Pétron, G., et al. (2012), Hydrocarbon emissions characterization in the Colorado Front Range: A pilot study, *J. Geophys. Res.*, *117*, D04304, doi:10.1029/2011JD016360.

Podolske, J. R. (2003), Calibration and data retrieval algorithms for the NASA Langley/Ames Diode Laser Hygrometer for the NASA Transport and Chemical Evolution Over the Pacific (TRACE-P) mission, *J. Geophys. Res.*, *108*(D20), 8792, doi:10.1029/2002JD003156.

Poisson, N., M. Kanakidou, and P. J. Crutzen (2000), Impact of non-methane hydrocarbons on tropospheric chemistry and the oxidizing power of the global troposphere: 3-dimensional modelling results, *J. Atmos. Chem.*, *36*, 157–230, doi:10.1023/A:1006300616544.

Poulida, O., R. R. Dickerson, and A. Heymsfield (1996), Stratosphere-troposphere exchange in a midlatitude mesoscale convective complet, *J. Geophys. Res.*, *101*, 6823–6836, doi:10.1029/95JD03523.

Price, J., and G. Vaughan (1993), The potential for stratosphere-troposphere exchange in cut-off-low systems, *Q. J. R. Meteorol. Soc.*, *119*(510), 343–365, doi:10.1002/qj.49711951007.

Riese, M., F. Ploeger, A. Rap, B. Vogel, P. Konopka, M. Dameris, and P. Forster (2012), Impact of uncertainties in atmospheric mixing on simulated UTLS composition and related radiative effects, *J. Geophys. Res.*, *117*, D16305, doi:10.1029/2012JD017751.

Sachse, G. W., and G. F. Hill (1987), Fast-response, high-precision carbon monoxide sensor using a tunable diode laser absorption technique, *J. Geophys. Res.*, *92*, 2071–2081, doi:10.1029/JD092iD02p02071.

Sachse, G. W., J. E. Collins, G. F. Hill, L. O. Wade, L. G. Burney, and J. A. Ritter (1991), Airborne tunable diode laser sensor for high-precision concentration and flux measurements of carbon monoxide and methane, in *Proceedings of the Society for Photo-Optical Instrumentation Engineers (SPIE)*, *Measurement of Atmospheric Gases*, vol. 1433, edited by H. I. Schiff, pp. 157–166 Los Angeles, Calif.

Simpson, I. J., et al. (2010), Characterization of trace gases measured over Alberta oil sands mining operations: 76 speciated C2–C10 volatile organic compounds (VOCs), CO_2, CH_4, CO, NO, NO_2, NOy, O_3, *Atmos. Chem. Phys.*, *10*(23), 11,931–11,954, doi:10.5194/acp-10-11931-2010.

Sive, B. C. (1998), *Atmospheric Nonmethane Hydrocarbons: Analytical Methods and Estimated Hydroxyl Radical Concentrations*, Univ. of Calif., Irvine.

Sprenger, M., H. Wernli, and M. Bourqui (2007), Stratosphere–Troposphere exchange and its relation to potential vorticity streamers and cutoffs near the extratropical tropopause, *J. Atmos. Sci.*, *64*(5), 1587–1602, doi:10.1175/JAS3911.1.

Stohl, A. (2003), Stratosphere-troposphere exchange: A review, and what we have learned from STACCATO, *J. Geophys. Res.*, *108*(D12), 8516, doi:10.1029/2002JD002490.

Stohl, A., H. Wernli, P. James, M. Bourqui, C. Forster, M. A. Liniger, P. Seibert, and M. Sprenger (2003), A new perspective of stratosphere–troposphere exchange, *Bull. Am. Meteorol. Soc.*, *84*(11), 1565–1573, doi:10.1175/BAMS-84-11-1565.

Trainer, M., B. A. Ridley, M. P. Buhr, G. Kok, J. Walega, G. Hiibler, D. D. Parrish, and F. C. Fehsenfeld (1995), Regional ozone and urban plumes in the southeastern United States: Birmingham, a case study, *J. Geophys. Res.*, *100*, 18,823–18,834, doi:10.1029/95JD01641.

Vaughan, G., J. D. Price, and A. Howells (1994), Transport into the troposphere in a tropopause fold, *Q. J. R. Meteorol. Soc.*, *120*(518), 1085–1103, doi:10.1002/qj.49712051814.

Vaughan, G., F. M. O. Connor, and D. P. Wareing (2001), Observations of Streamers in the Troposphere and Stratosphere Using Ozone Lidar, *J. Atmos. Chem.*, *38*, 295–315.

WHO (2005), WHO air quality guidelines global update 2005 global update, in *Report on a Working Group Meeting*, *Bonn*, *Germany*, *18–20 October 2005*.

WMO (1957), Meteorology—A three-dimensional science: Second session of the commission for aerology, *World Meteorol. Organ. Bull.*, *4*, 134–138.

World Meteorological Organization (WMO)/United Nations Environment Programme (UNEP) (2007), Scientific assessment of ozone depletion: 2006, WMO.

Zeng, G., O. Morgenstern, P. Braesicke, and J. A. Pyle (2010), Impact of stratospheric ozone recovery on tropospheric ozone and its budget, *Geophys. Res. Lett.*, *37*, L09805, doi:10.1029/2010GL042812.